Available online at www.sciencedirect.com
SCIENCE DIRECT®

Journal of the European Ceramic Society 24 (2004) 963–967

www.elsevier.com/locate/jeurceramsoc

The structure properties correlation in the Ce-doped SnO_2 materials obtained by different synthesis routes

S. Mihaiu*, G. Postole, M. Carata, M. Caldararu, D. Crisan, N. Dragan, M. Zaharescu

Romanian Academy, Institute of Physical Chemistry "I. G. Murgulescu" 202 Splaiul Independentei, 77208 Bucharest 6, Romania

Abstract

Ce-doped SnO_2 materials with rutile type structure ($SnO^{\bullet}_{2(SS)}$) were obtained as porous ceramic, powders and films from different precursor mixtures and by using different preparation routes. The samples were characterized in terms of their structural, morphological and electrical properties. Depending on the specific precursor mixture, different microstructural parameters were obtained. The lattice parameters of the host oxide (SnO_2) decrease by CeO_2 doping and the mean crystallite size D varies in the range of 670–1278 Å; different values of lattice strain S were also noticed. The morphological characteristics as shrinkage ($\Delta l/l$), porosity (Pa), density (d) and BET surface area were determined. The electrical properties were measured on the porous ceramics and on the powders. All investigated samples showed n-type semiconducting behavior.

Keywords: Ce-doped SnO_2; Electrical properties; Films; Microstructure; Powders

1. Introduction

Oxide materials belonging to the SnO_2–CeO_2 system are of great interest due to their use as solid electrolytes in fuel cells,[1] as catalysts,[2] sensors[3,4] and photoanodes for solar cells.[5]

The peculiar properties required by each of these applications can be controlled by varying the morphology of the materials (particle size, porosity and surface area) which in turn depends on the method of preparation.

Most of the papers published recently refer to powders and thin films mainly obtained by using aqueous colloidal solutions of inorganic salts, which are very stable.[3,5,6] However, in some of the cases, the inorganic anions could have a negative influence on the properties of the products; in these cases the alcoholic route of preparation using cerium and tin alkoxides is recommended.

This paper aims to obtain Ce-doped SnO_2 materials by (i) ceramic, (ii) thermal decomposition of inorganic salts and (iii) sol-gel alkoxides routes. Ceramics, powders and films obtained in this way were characterized in terms of their structural, morphological and electrical properties.

2. Experimental

2.1. Sample preparation

The reagent grade materials used for each different synthesis route to produce samples with the Sn:Ce atomic ratio as 97.5 : 2.5 were the following:

(a) SnO_2 (Merck) and CeO_2 (Lobo Feinchemie), in the ceramic method, resulting samples identified by abbreviation **CS**.
(b) Tin (II) oxalate (Merck) and cerium (IV) sulfate tetrahydrate (Lobo Feinchemie) or cerium (IV) ammonium nitrate (Lobo Feinchemie), in the thermal decomposition of inorganic salts method, resulting samples identified as **TD(I)** and as **TD(II)**, respectively (depending on the type of Ce-salt used).
(c) Sn (IV)-isopropoxide adduct in isopropanol (INORGTECH) and Ce(IV)-methoxy-ethoxide (laboratory synthesized) in sol-gel route (resulting the sample identified as **SGF**).

* Corresponding author. Tel.: +40-1638-53-70-26; fax: +40-1312-11-47.
E-mail address: smihaiu@chimfiz.icf.ro (S. Mihaiu).

0955-2219/03/$ - see front matter © 2003 Elsevier Ltd. All rights reserved.
doi:10.1016/S0955-2219(03)00398-4

The **CS** samples were obtained by classical ceramic method, by forming cylindrical pellets with a diameter of 10 mm and variable heights, which were thermally treated at 1000 and 1100 °C for 3 and 10 h.

The powders labeled as **TD(I)** and **TD(II)** were obtained by trituration during 30 min in an agate mortar of the precursor mixtures, which were thermally treated afterwards for 1 h at 950 °C for the sample **TD(I)** and at 500 °C for the sample **TD(II)**. Afterward, for a proper refinement of the XRD analysis, the obtained powders were thermally treated at 1000 °C for 3 h.

In order to obtain the **SGF** sample Sn(IV)-isopropoxide was dissolved in EtOH, previously treated with concentrated HNO_3 (at pH = 4) and Ce(IV)-methoxyethoxide was added. The as-obtained solution was mixed by stirring for 1 h in a closed system. The Ce-doped SnO_2 supported films on silicon wafer substrates have been obtained by dip coating. After drying in air for 24 h the films were thermally treated at 850 °C.

2.2. Sample characterization

The thermal behavior of precursors and of the final products was analyzed by DTA/TG measurements (with MOM-OD-103 Derivatograph) up to 1350 °C with a linear heating rate of 7.5 °C/min.

XRD analysis of the samples was performed with a TUR M-62 instrument equipped with a HZG-3 Diffractometer operating with Co K_α radiation. For the refinement of the XRD structural characterisation a step by step analysis ($\theta = 0.01°$) has been done. The unit cell lattice parameters, the crystallites mean size (D), the lattice strain (S) and the scattering of the shape factor ($\Delta\Phi$) were calculated by using the XRAY 3.0 program (an improved variant of the XRAY 1.0).[7]

IR absorption measurements were performed by using KBr containing pellets on IR M-80 Carl Zeiss spectrometer between 1600 and 400 cm^{-1}.

The morphological characteristics, namely shrinkage ($\Delta l/l$), porosity (Pa) and density (d) and the BET surface areas were also determined.

The dc electrical properties of the **CS** was measured by the four points method [8] between 2 and 850 °C. The ac electrical conductivity of **TD(I)** and **TD(II)** powders was measured in situ in a specially designed cell (with two coaxial cylindrical electrodes, the non-pressed powder filling the annular space) described elsewhere [9] and the differential step technique; it consists essentially in comparing the results of repeated thermal cycling between 20 and 400 °C (by linear heating, 2 °C/min) of the same batch while flushing with various gases and monitoring the composition of the effluent.[9] Thus, the changes of conductivity can be directly associated with dehydration, gas adsorption, oxidation/reduction, etc. The succession of cycles was: DAr-1 to 3, DO, CT, DAr-4 (after the catalytic test), where DAr and DO represent dry argon and dry oxygen, respectively, and CT represents the mixture used for the catalytic test (propylene: air 1:10).

3. Results and discussion

3.1. Thermal behavior

The results of the DTA/TG analysis are presented in Table 1. According to our previous investigations, the **CS** precursors (SnO_2 and CeO_2) do not show weight loss and thermal effects in the investigated temperature range.[8] Tin (II) oxalate decomposes up to 390 °C leading to SnO_2 formation. $(NH_4)_2Ce(NO_3)_6$ decomposes up to 415 °C with the formation of CeO_2, while the decomposition of $Ce(SO_4)_2\times4H_2O$ is completed only at about 930 °C.

As expected, $SnO_2 + CeO_2$ mixtures do not loose weight between 20 and 1500 °C, i.e. in the temperature range used for the preparation of the **CS** sample.

Table 1
The results of the DTA/TG analysis of the investigated reaction mixtures

No	Sample	Starting compounds	Temp. range (°C)	Mass variation		Phase[a] composition
				%exp	%calc	
Precursors						
1	SnC_2O_4	SnC_2O_4	320–390	−29.41	−27.01	SnO_2
2	$CeH_8N_8O_{18}$	$(NH_4)_2Ce(NO_3)_6$	190–415	−71.75	−68.86	CeO_2
3	$CeH_8S_2O_{12}$	$Ce(SO_4)_2\times4H_2O$	180–930	−56.8	−57.43	CeO_2
Reaction mixtures						
4.	CS	$SnO_2 + CeO_2$	20–1500	No variation		SnO_2
5.	TD(I)	$SnC_2O_4 + Ce(SO_4)_2\times4H_2O$	200–853	−30.51	−28.54	SnO_2
6.	TD(II)	$SnC_2O_4 + (NH_4)_2Ce(NO_3)_6$	100–390	−31.02	−29.74	SnO_2
7.	SG[b]	$Sn(iOC_3H_7)_4 + Ce(OCH_3)_2(OC_2H_5)_2$	40–450	−19.21	–	SnO_2

[a] ATD residues at 1000 °C (for CS 1500 °C).
[b] Gel dried in air resulted from solution used for films deposition.

For the precursor mixture of the **TD(I)** sample, the formation of the oxide mixture (SnO_2+CeO_2) was complete at 853 °C (i.e. almost 80 °C less than the final temperature of decomposition of cerium precursor $Ce(SO_4)_2\times4H_2O$). The onset temperature for the decomposition of the precursor mixture of the **TD(II)** sample was lower in comparison with that of the corresponding tin precursor [tin (II) oxalate] but the decomposition ends at the same temperature (390 °C).

The temperature up to which the mass variation of the **SG** sample takes place (450 °C) is similar for other SnO_2 based gels obtained in ethyl alcohol media.[10]

The conditions of the thermal treatments applied for the samples (Table 2) were selected based on the results of thermal analysis.

3.2. Structural characterization

Some structural characteristics of the host (SnO_2) and of the dopant (CeO_2) oxides are presented in Table 3. According to literature data,[11,12] SnO_2 presents a tetragonal structure (P_4/mm space group). CeO_2 has a cubic structure (Fm3m space group). The coordination number is 6 for SnO_2 and 8 for CeO_2.

Phase composition of all samples (Table 2) shows only one phase $SnO_{2(SS)}$. The **TD(II)** and **SGF** samples, thermally treated at 500 and 850 °C respectively show a low degree of crystallization. The microstructural parameters could be calculated only for the **CS**, **TD(I)** and **TD(II)** samples thermally treated at 1000 °C.

In Table 3 the lattice parameters, unit cell volume, the mean crystallite size (D), the lattice strain (S) and the scattering of the shape factor ($\Delta\Phi\%$) are presented. A decrease of the lattice parameters of the host oxide (SnO_2) by doping with CeO_2 is in evidence. The calculated values of the mean crystallite size (D) are in the 670–1278 Å range in good agreement with reference data.[6] Different values of the lattice strain (S) were obtained for each distinct composition of precursors. The smallest value of 0.4×10^{-3} was found for the **TD(I)** sample, while the highest value of 1.1×10^{-3} was obtained for the **CS** sample. Distinct values for each mixture of precursors have also been obtained for the scattering of the shape factor ($\Delta\Phi\%$).

Table 2
Thermal treatment schedule of the studied samples

Sample	Temp. (°C)	Phase composition	Temp. (°C)	Phase composition
CS	1000	$SnO_{2(SS)}$	1100	$SnO_{2(SS)}$
TD(I)	950	$SnO_{2(SS)}$	1000	$SnO_{2(SS)}$
TD(II)	500	SnO_2 low crystallization	1000	$SnO_{2(SS)}$
SGF	500	SnO_2 low crystallization	850	$SnO_{2(SS)}$

Table 3
Microstructural parameters calculated from X-ray diffraction data for the samples thermally treated at 1000 °C

Sample	Lattice parameters			D (Å)	$S\times10^3$	$\Delta\Phi$ (%)
	a (Å)	c (Å)	V(Å^3)			
CeO_2 (ASTM)	5.4113	–	158.46			
CeO_2	5.4071	–	158.08(7)	1278	0.3	1.8
CS	4.7286	3.1841	71.19(3)	670	1.1	2.1
TD(I)	4.7305	3.1832	71.23(1)	827	0.4	3.4
TD(II)	4.7324	3.1826	71.28(1)	805	0.7	2.7
SnO_2	4.7334	3.1846	71.35(1)	1133	0.6	4.2
SnO_2 (ASTM)	4.7380	3.1880	71.57			

In Fig. 1 the IR spectra of the **CS** and **TD(I)** and **TD(II)** samples thermally treated at 1000 °C in comparison with the pure SnO_2 are presented. A flattening of the bands characteristic for pure SnO_2 lattice and even the disappearance of the band at 680 cm^{-1} was observed for Ce-doped compounds. This suggests the substitution of Sn^{4+} by Ce^{4+} ions in all studied samples. By this substitution, the Ce^{4+} ions are compelled to adopt octahedral coordination which is unusual for this ion. This fact explains the strong distortion of the Ce-doped SnO_2 and the decrease of unit cell volume.

3.3. Morphology of the samples

The morphological characteristics for materials studied by electrical conductivity are shown in Table 4. The high value of the apparent porosity ($Pa=9$), the increase of diameter ($\Delta l/l=+1$) of the samples after the thermal treatment and the low value of relative density ($d_r=63.11\%$) as well indicate the formation of porous ceramics.

The values of BET surface area of **TD(I)** and **TD(II)** powders are similar to those reported in references,[6] depending on the type of precursors used and on the

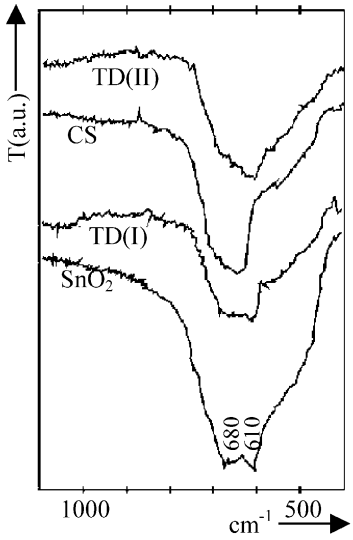

Fig. 1. The IR spectra of the samples thermally treated at 1000 °C.

thermal treatment applied. In the case of the **TD(II)** sample the particles are below 20 nm.

3.4. Electrical properties

The electrical properties were measured on the **CS** porous ceramics and on the **TD(I)** and **TD(II)** powders. The variation of $\ln\sigma$ versus $1000/T$ presented in Fig. 2 for the **CS** sample indicated two different slopes, separated by a maximum in the 127–287 °C temperature range. Such a behavior was also noticed in other experiments on oxygen adsorption on pure SnO_2 and was associated with water desorption.[13] The two different activation energies may be assigned to two different conduction mechanisms, due to the migration of charge carriers in presence of pores.[14] Fig. 3 presents for comparison the variation with temperature of the ac apparent conductivity for **TD(I)** and **TD(II)** on heating in DAr (1 and 3), DO and in DAr-4 (after the catalytic test) runs. Both samples lose water on dry argon flushing/heating (Fig. 4). The progressive dehydration is accompanied by the decrease of conductivity(see DAr-1 versus DAr-3), indicating an important contribution of protonic conduction [15] on wet samples. The initial loss of water was more important for the **TD(II)** sample

Table 4
The morphological characteristics of the samples used for electrical measurements

Sample	Thermal treatment	Materials	Morphology
CS	1100 °C, 10 h	Porous ceramic	$Pa = 9.0\%$ $\Delta l/l = +1$ $d_l = 63.11\%$
TD(I)	950 °C, 1 h	Powders	Ssp area (BET) = 5 $m^2\ g^{-1}$ $D = 778$
TD(II)	500 °C, 1 h	Powders	Ssp area (BET) = 47 $m^2\ g^{-1}$ $D = 177$

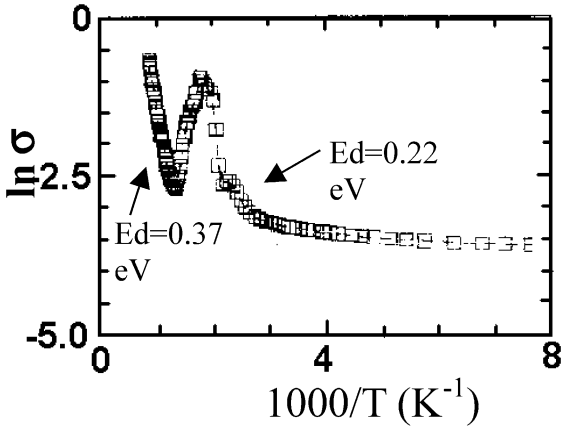

Fig. 2. The variation of ln σ versus $1000/T$ in the 2–850 °C temperature range for the porous ceramic (**CS**) sample.

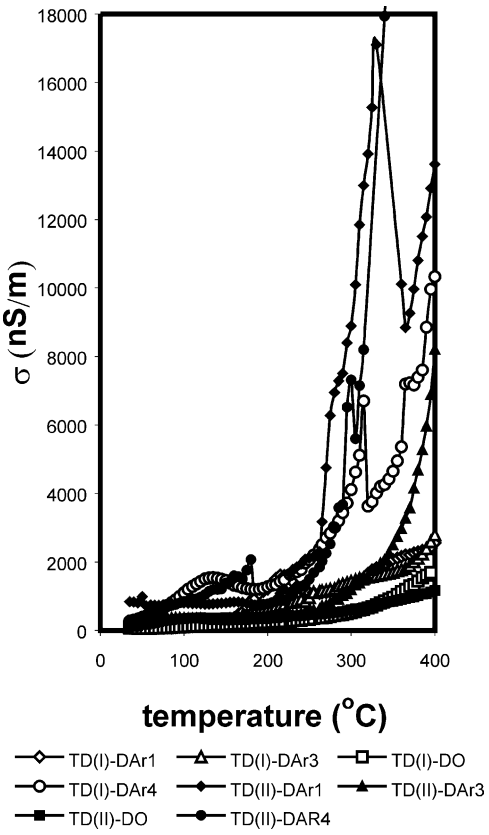

Fig. 3. The variation with temperature of the ac apparent conductivity for **TD(I)** and **TD(II)** samples on heating in dry argon (DAr1 and 3), in dry oxygen (DO) and DAr-4 (after the catalytic test).

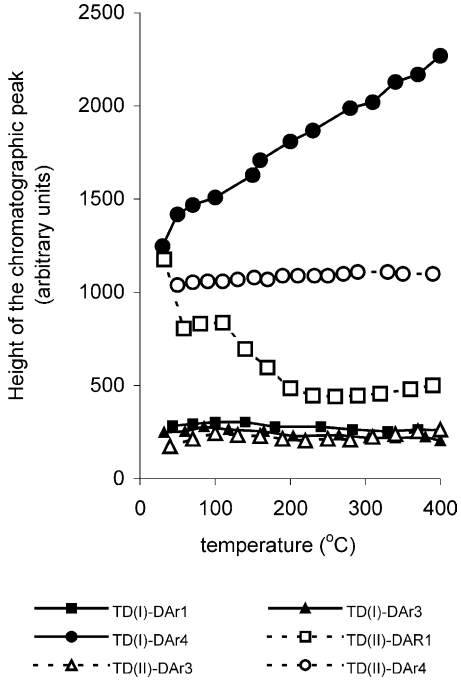

Fig. 4. Water evolution in effluent during heating of the **TD(I)** and **TD(II)** samples in dry argon (DAr1 and 3) and DAr-4 (after the catalytic test).

(calcined at lower temperature) and considerably higher for both after the catalytic test. The higher values (particularly at high temperature) for **TD(II)** indicate a higher level of disorder, supported also by the higher decrease of σ in oxygen (as expected for *n*-type semiconductors). The plots show also essentially 2 regimes; the transition temperature (250 °C) coincides with the onset of the catalytic activity. Based on the higher increase of conductivity in DAr-4, **TD(II)** sample (dominantly amorphous, as proved by XRD analysis) seems to be also more reducible during the catalytic test than **TD(I).**

4. Conclusions

Ce-doped SnO_2 with rutile structure were obtained as porous ceramics, powders and films by using different synthesis routes and different precursor mixtures.

Microstructural parameters calculated from X-ray diffraction data present different values according to the distinct mixtures of the precursors.

The porous ceramics and the powders present n-type semiconducting behavior. A good correlation between morphological characteristics and electrical properties was found.

The powders obtained by thermal decomposition of the inorganic salts with nanometer size of the grains seem to be promising catalysts for hydrocarbon combustion.

References

1. Feng, M. and Goodenough, J. B., A superior oxide-ion electrolyte. *Eur. J. Solid State Inorg. Chem*., 1994, **T31**, 663–672.
2. Sasikala, R., Gupta, N. M. and Kulschreshtha, S. C., Temperature-programmed reduction and CO oxidation studies over Ce–Sn mixed oxides. *Catal. Lett*., 2001, **71**(1-2), 69–74.
3. Fang, G., Liu, Z., Liu, C. and Yao, K. L., Room temperature H_2S sensing properties and mechanism of CeO_2–SnO_2 sol-gel thin films. *Sens. Actuators, B*, 2000, **B66**(1-3), 46–48.
4. Jyothi, T. M., Talawar, M. B. and Rao, B. S., Formation of anisaldehyde via hydroxymethylation of anisole over SnO_2–CeO_2 catalysts. *Catal. Lett*., 2000, **64**(2-4), 151–155.
5. Turcovic, A. and Crnjacorel, Z., Dye-sensitized solar cell with CeO_2 and mixed CeO_2/SnO_2 photoanodes. *Sol. Energy Mater. Sol. Cells*, 1997, **45**(3), 275–281.
6. Azelee, W. and Harrison, G. Ph., Investigation of the pore texture of SnO_2–CeO_2 composite oxides. *J. Sol-Gel. Sci. Technol*., 1997, **9**, 41–53.
7. Dragan, N., Profile fitting procedure using least-squares and integral breadth method for fast analysis of broadening X-ray diffraction peaks. In *6th National Conference of the Bulgarian Catalysis Club*, 1999, p. 10.
8. Mihaiu, S., Scarlat, O., Aldica, Gh. and Zaharescu, M., SnO_2 electroceramics with various additives. *J. Eur. Ceram. Soc*., 2001, **21**, 1801–1804.
9. Caldararu, M., Spranceana, D., Popa, V. T. and Ionescu, N. I., Surface dynamics in tin dioxide-containing catalysts. II. Competition between water and oxygen adsorption on polycrystalline tin dioxide. *Sensors and Actuators B*, 1996, **30**, 35–41.
10. Savaniu, C., Arnãutu, A., Cobianu, C., Crãciun, G., Flueraru, C., Zaharescu, M., Pârlog, C., Paszti, F. and Van den Berg, A., Tin dioxide sol-gel derived films doped with platinum and antimony deposited on porous silicon. *Thin Solid Films*, 1999, **341**, 1–7.
11. Jarzebski, Z. M. and Marton, J. P., Physical properties of SnO_2 materials. 1. Preparation and defect strucure. *J. Electrochem. Soc*., 1976, **123**(7), 199–205C.
12. Wyckoff, R. W. G., *Crystal Structures*. John Wiley & Sons, New York, 1964.
13. Caldararu, M., Mihaiu, S., Spranceana, D., Zaharescu, M., Popa, V. T. and Ionescu, N. I., The role of hydration-dehydration effects on oxygen adsorption on SnO_2. *Rev. Roum. Chim*., 1999, **44**(11-12), 1121–1127.
14. Mihaiu, S., Scarlat, O., Aldica, Gh. and Zaharescu, M. Electrical properties of the ceramics from the SnO_2–$CuSb_2O_6$ pseudobinary system. Presented at 10th International Ceramics Congress and 3th Forum on New Materials (CIMTEC-2002) Florence, Italy, 14–18 July, 2002.
15. Caldararu, M., Postole, G., Hornoiu, C., Bratan, V., Dragan, M. and Ionescu, N. I., Electrical conductivity of γ-Al_2O_3 at atmospheric pressure under dehydrating/hydrating conditions. *Appl. Surf. Sci*., 2001, **181**(3-4), 255–264.